17th World Conference on Earthquake Engineering, 17WCEE
Sendai, Japan - September 27th to October 2nd, 2021

IN-PLANE SEISMIC RESPONSE OF FULL-SCALE EARTHEN WALLS IN HISTORIC CONSTRUCTION

J. C. Reyes[(1)], L. E. Yamin[(2)], W. M. Hassan[(3)] , J. P. Smith-Pardo[(4)], J. D. Sandoval[(5)], C. D. Gonzalez[(6)], and F. A. Galvis[(7)]

[(1)] *Associate Professor, Universidad de los Andes, Bogotá, Colombia, jureyes@uniandes.edu.co*
[(2)] *Associate Professor, Universidad de los Andes, Bogotá, Colombia, lyamin@uniandes.edu.co*
[(3)] *Associate Professor, University of Alaska, Anchorage, AK, USA, wmhassan@alaska.edu*
[(3)] *Associate Professor, Housing and Building National Research Center, Giza, Egypt, whassan@berkeley.edu*
[(4)] *Associate Professor, Seattle University, Seattle, WA, USA, smithjh@seattleu.edu*
[(5)] *Graduate research assistant, Universidad de los Andes, Bogotá, Colombia, jd.sandoval3153@uniandes.edu.co*
[(6)] *Graduate research assistant, Universidad de los Andes, Bogotá, Colombia, cd.gonzalez2248@uniandes.edu.co*
[(7)] *Ph.D. candidate, Stanford University, Stanford, USA, galvisf@stanford.edu*

Abstract

Thick adobe and rammed earth walls are common features of traditional earthen construction in many parts of the world, including the colonial period construction in South America and most sites in the World Heritage's List. Furthermore, about one third of the world's population live in earthen houses. During past earthquakes, existing earthen buildings have shown severe vulnerability and suffered substantial damage or collapse leading to fatalities and major economic and cultural losses. Poor mechanical properties, small in-plane capacity, out-of-plane instability, lack of seismic diaphragms, and low strength of the connections between structural elements are characteristic in such construction. This paper presents the results of a comprehensive experimental campaign conducted to characterize the in-plane seismic response of thick earthen walls and investigate several seismic retrofit schemes to mitigate severe seismic damage or collapse risk. The study presents the test results of 19 full-scale adobe and rammed earth (RE) walls cyclically loaded in-plane with displacement reversals. The test parameters include the type of earth materials, axial load, wall aspect ratio, effect of wall openings, the type of retrofitting material and system. The three proposed retrofitting schemes are: steel straps, flexible steel welded wire mesh and a combination of vertical and horizontal timber straps along with post-tensioned rods. The test specimens include 10 bare or unretrofitted specimens (6 adobe and 4 RE walls) to characterize the seismic performance and evaluate shear strength and 9 specimens (5 adobe and 4 RE walls) to quantify the feasibility of the proposed retrofitting alternatives. Test results of the unretrofitted walls show that the failure mechanisms are dominated by the presence of diagonal cracks that divide the walls into large segments that eventually fall off jeopardizing shear capacity. The results also showed that shear capacity is controlled by the wall axial load and aspect ratio. The unretrofitted walls and wall piers had lower bounds of local drift capacity at initial cracking and peak shear strength of 0.08% and 0.80%, respectively and a global drift capacity of 0.55%. Steel straps retrofit increased adobe wall lateral strength and deformation capacity by 30% and 380%, respectively, allowing drift capacity to reach 5.3%. Flexible steel wire mesh marginally increased shear strength of adobe walls under high axial load, while it was efficient enhancing shear strength under low axial load by about 3 times the bare wall strength; in contrast to an average strength enhancement of 42% in RE walls. The flexible steel wire mesh was ineffective in enhancing drift capacity of both adobe and RE walls under high axial load, while it improved the adobe wall drift capacity by 2-3 times. The third retrofit solution featuring a combination of vertical and horizontal timber straps along with post-tensioned rods provided superior performance to the retrofitted adobe and RE walls with openings, enhancing the lateral strength of these walls by about 70% with the respect to the unretrofitted walls. Furthermore, this retrofit solution increased the drift capacity of both adobe and RE walls with openings by more than 5 times, surpassing 2.5% drift ratio.

Keywords: earthen walls; cyclic tests; in-plane seismic response; shear walls; adobe and rammed earth.

1. Introduction

It has been reported that between one third and one half of the world's population still live on dwellings made earthen materials [1, 2]. According to UNESCO [3], more than 150 of the World Heritage sites have been constructed with earth. The clear popularity of earthen materials through human development is due to a combination of factors such as availability, low cost, environmentally friendliness, intrinsic ability to provide thermal and noise insulation, as well as moisture regulation. However, the main caveat is that earthen components are massive, brittle, an often poorly detailed/engineered thus rendering them very vulnerable to earthquake damage and collapse [4-6]. Research has emerged in recent years on the development of non-engineered retrofitting techniques for earthen construction such as using straps from used car tires [7], polypropylene (PP) bands [8], or polyester fabric strips [9], which have resulted in promising improvements on the seismic behavior. Nevertheless, the vast number of experimental and numerical studies that are available in the literature often focus on reduced scale models of single walls or houses and a limited number of full-scale solid walls. Unfortunately, the number of studies dealing with full-scale walls with openings, representative of what can be expected in the field, are rather scarce.

In addition to the obvious concern of life safety, preservation of historical value of some of the earthen construction cannot be understated. Thick adobe and rammed earth walls are typical features of heritage construction from the colonial period of South America. Though strengthening of cultural buildings in Colombia has taken place over decades, consistent documentation of implemented solutions and development of guidelines and code provisions had not emerged. This combined with a growing awareness of seismic risk to the country's heritage inventory led the Colombian Ministry of Culture partner with the Colombian Association of Earthquake Engineering and the Universidad de Los Andes to conduct a comprehensive multi-phase experimental study aimed at investigating the seismic behavior of thick earthen walls. This paper presents relevant results of a subset of specimens subjected to in-plane loading along with the experimental evaluation of their response with and without retrofitting using engineered and non-engineered materials. Full scale test results of thick walls piers (between consecutive doors or between a door and a window) and entire wall segments with door and window openings are presented in this paper to contribute to much needed experimental data on the seismic behavior of unretrofitted and retrofitted heritage infrastructure [10-13].

2. Materials

The wall test specimens in this study were built using older earthen material blocks extracted from 100-year old earthen buildings scheduled for demolition in Colombia. Soil from a the demolished heritage building complex was extracted, cleaned and used as mortar for the adobe walls and earth for the RE walls specimens. The material physical and mechanical properties were determined based on standard tests. Additionally, compression and bending tests of adobe and RE individual bricks as well as compression tests on 140×280×320mm brick prisms were performed. Diagonal tension tests were performed using square wall panels 700×700×280mm and 1000×1000×400mm for adobe and RE, respectively. Results from the earthen material mechanical characterization tests are presented in [10-13] and summarized in Table 1 for completeness and expedite reference.

The mechanical properties of the A36 steel plates (6.35-mm-thick) were verified by three ASTM A370 tests. The average Young modulus was 224,000 MPa, and the mean yield and ultimate strength were 293 MPa and 362 MPa, respectively. The 9.53-mm diameter steel bars had an average yielding stress of 430 MPa (per ASTM A307). The tensile strength of the flexible steel welded wire mesh (FSWM) used as a second retrofitting alternative was measured in according to ASTM A370 yielding a median tensile strength of 518 MPa. The exterior and exterior meshes were connected to each other using 8.0 mm-diameter steel wires through previously drilled holes at 500 mm spacing. Tensile tests of the 8 mm wires rendered yielding and ultimate strengths of 430 MPa and 488 MPa on average for the steel material.

Table 1 – Material characterization test results

Specimen description	Mechanical property measured	Number of Specimens	Median capacity [kN/m^2]	COV
Adobe unit	Compression	33	2800	0.30
	Modulus of rupture	7	480	0.36
140×280×320mm adobe prism	Compression	6	1350	0.14
140×280×320mm RE prism	Compression	5	1100	0.08
700×700×280mm adobe panel	Diagonal tension	10	27	0.28
1000×1000×400mm RE panel	Diagonal tension	13	31	0.38

3. Experimental program

A comprehensive experimental program was executed to build and test nineteen full-scale adobe and RE wall specimens under quasi-static cyclic displacement reversals with the purpose of quantifying their in-plane seismic response under the effect of several influential parameters and proposed retrofitting techniques.

3.1 Specimen description

Table 2 presents the details of the 19 test specimens. The test specimens were classified in three groups based on the wall aspect ratio , which is the quotient between the wall height and its length. The first group comprises solid specimens B1, B2, and B3 measuring 1.25×2.35×0.6 m with an aspect ratio of 1.88 and representing the wall pier between a door and a window [11]; the second includes solid specimens measuring 2.5×1.8×0.4 m with an aspect ratio of 0.72 and representing the wall pier between two doors [10, 12]. The third group consists of perforated walls representing a portion the façade in a one-story house, including a door and a window opening [10, 12, 13]. The walls have overall dimensions of 7.00×3.45×0.60 m and an aspect ratio of 0.49. The geometry of the wall test specimens is depicted in Fig. 1 (unretrofitted counterparts are not shown). The walls were built by an experienced local contractor to represent traditional practices in Colombia. The solid wall specimens were constructed on a rock bed to simulate actual foundation conditions. The actual connection between the roof and the top of the wall was represented with a steel beam placed on timber elements in contact with the wall. The axial load of the solid walls B1, B2, B3 was applied using concrete blocks to simulate a tributary weight of 15 kN. The axial load of the solid walls in the second group was applied with a hydraulic jack mounted on a rolling mechanism on the top of a rigid steel beam. Three axial load levels of P = 70 kN (high), 50 kN (moderate), and 20 kN (small), were evaluated for this second group to cover a range of tributary loads for one- and two-story structures. The specimens with openings in the third group included the effect of adjacent walls by adding two short buttresses perpendicular to the main wall. The foundation of the specimens consisted of a channel shape reinforced concrete beam that simulated the confinement conditions at the ground level. The axial load of the walls with openings was applied as a vertical load of 51.9 kN using seven concrete blocks that represented the weight of a typical roof of this type of construction.

3.2 Retrofitting Schemes

Three proposed retrofitting schemes were assessed using cyclic tests of adobe and RE walls:

- Steel strap (SS) retrofitting: three full-scale 1.25×2.35×0.60 m adobe wall piers in the first specimen group were tested under in-plane cyclic loading, two unretrofitted B1, B2 and one retrofitted B3 specimen. The retrofitted specimen B3 had vertical and horizontal steel plates (6.35-mm thick by 101.6-mm width) located on both faces of the wall as shown in Fig. 1a. The steel plates were connected through the thickness of the specimen by 9.53-mm diameter rods located inside unfilled holes. The steel

plates and rods were welded together. Detailed information on the test setup, the installation procedure of the steel retrofitting straps, and the construction sequence can be found in Reyes et al. [11].

- Flexible steel welded wire mesh (FSWM) retrofitting: six retrofitted full-scale adobe and RE walls, 2.5×1.8×0.4 m, were built and tested under in-plane cyclic displacements to compare their responses to the six unretrofitted counterparts in the second specimen group. The specimens were retrofitted prior to testing by means of a flexible steel welded wire mesh placed on the inside and outside faces of the wall (Fig. 1b). The mesh was made of wires of 0.91 mm-diameter spaced at 25 mm in each direction and was attached using 29 mm-diameter metallic soda caps nailed to the earthen walls every 300 mm. The mesh did not cover the entire vertical surfaces of the wall, but instead it was placed on 0.45 m-horizontal strip at the top and two 0.75 m-wide vertical strips at the vertical edges of the specimens to mimic the beam and columns of a frame as illustrated in Fig. 1. Construction procedures and further details of these test specimens can be found in Reyes et al. [12].
- Timber straps and vertical post-tensioning steel rod (TSPR) retrofitting: upon completion of the cyclic tests of the unretrofitted adobe and RE wall specimens with openings (up to 0.46% drift) of the third group, the damaged wall specimens were retrofitted with timber straps and vertical post-tensioning rods as shown in Fig. 1c. Cracks were first filled with a lime-sand mortar then carving the earthen material to create recesses for the placement of timber straps. Finally, vertical post-tensioning steel rods were installed and tightened. Timber straps with dimensions of 180 mm wide by 40 mm thick were placed vertically and horizontally along the perimeter of the wall and around window and door openings (Fig. 1). In addition, intermediate straps were installed to ensure a maximum spacing (horizontal or vertical) of 1.2m following the recommendations from a previous research program conducted at the Universidad de los Andes [12]). Intersecting straps were connected using a 9.5mm-diameter through bolts along with two steel plates and screws. More detailed information about this retrofitting scheme can be found in Reyes et al. [13].

Table 2 – Test specimen details.

Specimen group	Specimen ID	Dimensions, m $l_w \times h_w \times t$	Wall type	Wall material	Aspect ratio α	Axial load kN	Retrofit scheme
Group 1	B1	1.25×2.35×0.60	Un-retrofitted	Adobe	1.88	15.0	-
	B2	1.25×2.35×0.60	Un-retrofitted	Adobe	1.88	15.0	-
	B3	1.25×2.35×0.60	Retrofitted	Adobe	1.88	15.0	SS
Group 2	A1-U	2.50×1.80×0.40	Un-retrofitted	Adobe	0.72	70.0	-
	A2-U	2.50×1.80×0.40	Un-retrofitted	Adobe	0.72	50.0	-
	A3-U	2.50×1.80×0.40	Un-retrofitted	Adobe	0.72	20.0	-
	A1-R	2.50×1.80×0.40	Retrofitted	Adobe	0.72	70.0	FSWM
	A2-R	2.50×1.80×0.40	Retrofitted	Adobe	0.72	50.0	FSWM
	A3-R	2.50×1.80×0.40	Retrofitted	Adobe	0.72	20.0	FSWM
	RE1-U	2.50×1.80×0.40	Un-retrofitted	Rammed earth	0.72	70.0	-
	RE2-U	2.50×1.80×0.40	Un-retrofitted	Rammed earth	0.72	50.0	-
	RE3-U	2.50×1.80×0.40	Un-retrofitted	Rammed earth	0.72	20.0	-
	RE1-R	2.50×1.80×0.40	Retrofitted	Rammed earth	0.72	70.0	FSWM
	RE2-R	2.50×1.80×0.40	Retrofitted	Rammed earth	0.72	50.0	FSWM
	RE3-R	2.50×1.80×0.40	Retrofitted	Rammed earth	0.72	20.0	FSWM
Group 3	A4-Open-U	7.00×3.45×0.60	Un-retrofitted	Adobe	0.49	51.9	-
	A4-Open-R	7.00×3.45×0.60	Repaired/retrofitted	Adobe	0.49	51.9	TSPR
	RE4-Open-U	7.00×3.45×0.60	Un-retrofitted	Rammed earth	0.49	51.9	-
	RE4-Open-R	7.00×3.45×0.60	Repaired/retrofitted	Rammed earth	0.49	51.9	TSPR

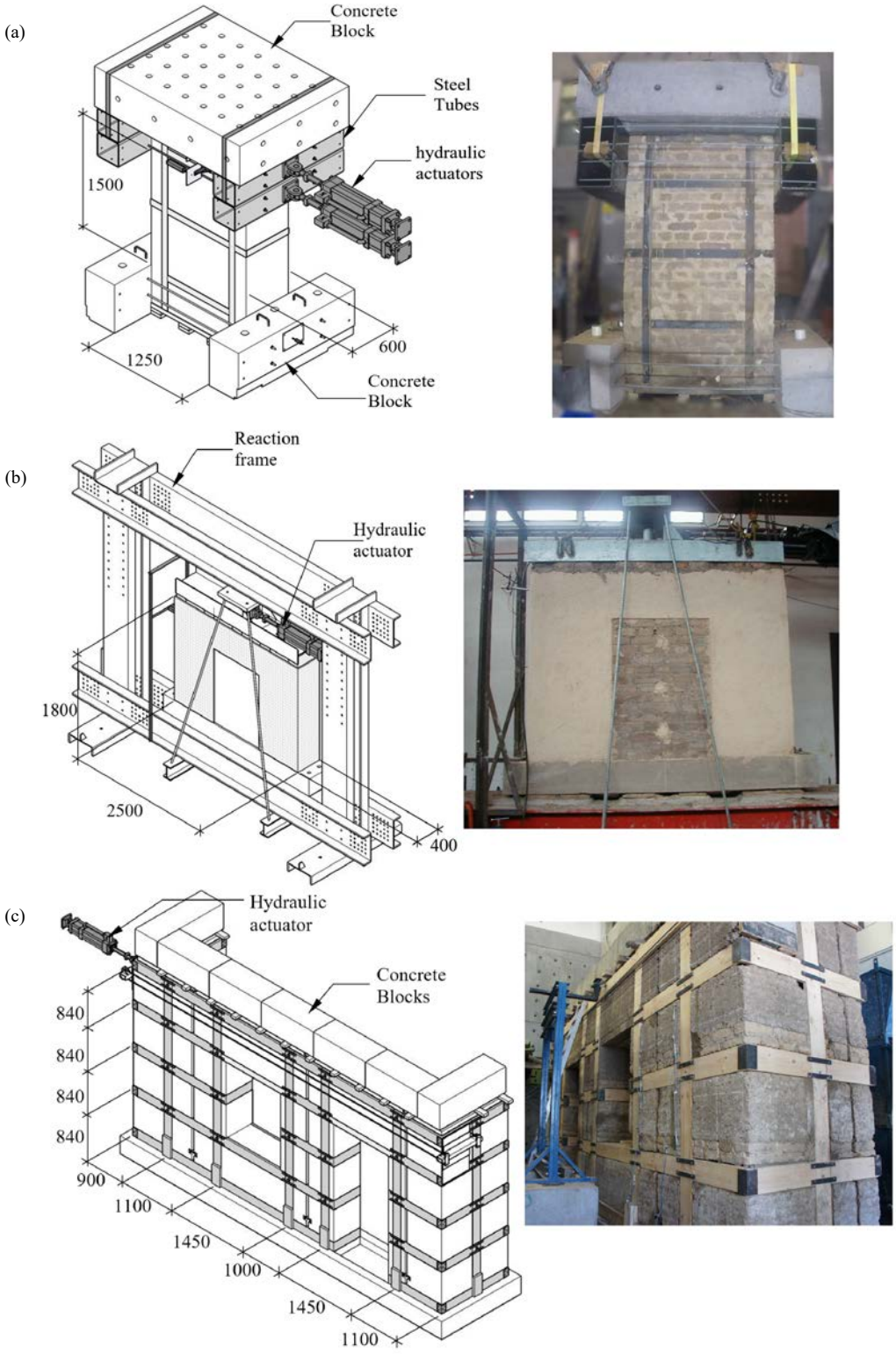

Fig. 1 – Test setup (unretrofitted counterparts not shown): (a) wall pier between window and door (Group 1); (b) wall pier between doors (Group 2); (c) wall façade with openings (Group 3).

3.3 Test setup, loading protocol and instrumentations

The test setup of Group 1 wall specimens is shown in Fig. 1a. Two parallel hydraulic actuators were used to apply the lateral displacement protocol shown in Fig. 2, which was based on FEMA 461 [14]. This protocol began with cycles of 0.20 mm amplitude (equivalent to 0.0056% drift) that were subsequently increased by a factor of 1.40 every two cycles.. The two hydraulic actuators were arranged to prevent the upper part of the specimen from rotating (Fig. 1). To reproduce fixed-fixed boundary conditions mimicking a double-curvature wall pier between a window and a door, the test setup included a lower and an upper 0.55m restriction zones by using concrete blocks and four HSS square steel tubes respectively. The steel straps of the retrofitted specimens of this group were instrumented with electric strain gauges.

A 350 kN hydraulic actuator located on the top of the steel beam applied the horizontal cyclic load for specimens in Group 2 as shown in Fig. 1b. Their axial load was applied with a hydraulic jack mounted on a rolling mechanism on the top of a rigid steel beam. Axial load was not applied simultaneously to the lateral load. The Group 2 walls were fully restrained against rotation at their base and free to rotate at the top, featuring a single-curvature situation which might pose a practical limitation. The cyclic tests of Group 2 were controlled by the displacement of an LVDT transducer located on the top-left corner of the walls; however, due to local damage at the controlling sensor location, only the load-displacement backbone curves were accurately recorded. The tests were displacement-controlled and following the protocol shown in Fig. 2. Tests were continued until the verge of lateral instability of the walls.

The perforated walls in Group 3 were cyclically loaded using a 350 kN hydraulic actuator connected to the laboratory reaction wall as shown in Fig. 1c. The actuator was attached to the wall by two steel devices, one at each end of the wall, and four rods that spanned between them, transferring the lateral load through a variable-depth plate to avoid stress concentrations. The Group 3 walls were subjected to the cyclic displacement protocol shown in Fig. 2. The test was stopped soon after the peak force started to decay because the main purpose of the program was to reach significant but repairable damage rather than collapse. The instrumentation of Group 3 walls featured 18 LVDT's to capture local and global deformations along with the internal bearing loading cell of the actuator.

4. Selected test results

Due to space limitations, Table 3 presents only selected test results representing the in-plane cyclic performance of the 19 test specimens featured in this comprehensive testing program. Damage patterns and in-plane force-displacement response are shown in Fig. 3 for Group 1, Figs. 4 and 5 for Group 2, and Fig. 6 for Group 3. For full sets of elaborate test results, the reader is referred to Reyes et al. [10-13].

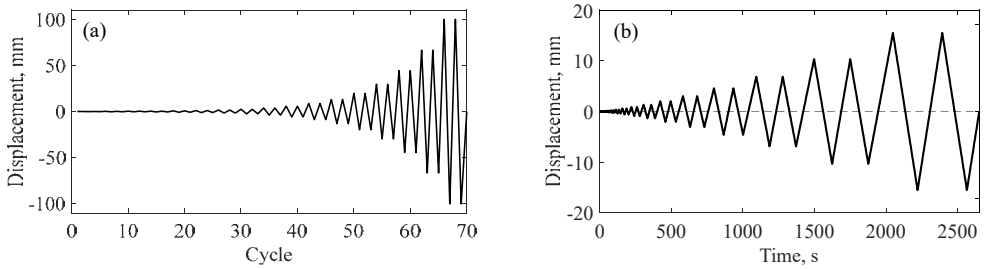

Fig. 2 – Displacement protocol (a): Group 1 and 3 specimens; (b) Group 2 specimens.

Table 3 – Test specimen partial results.

Specimen group	Specimen ID	Peak shear stress (kPa)	Drift at peak stress (%)	Maximum drift (%)
Group 1	B1	45.6	0.90	1.40
	B2	45.7	0.90	1.40
	B3	59.3	2.30	5.30
Group 2	A1-U	43.8	1.65	2.07
	A2-U	23.3	0.80	1.11
	A3-U	14.2	1.19	1.98
	A1-R	45.1	1.88	2.33
	A2-R	39.4	2.41	2.95
	A3-R	41.6	2.32	3.98
	RE1-U	33.0	1.68	1.74
	RE2-U	29.8	1.00	1.39
	RE3-U	17.3	1.82	2.88
	RE1-R	45.4	1.55	1.80
	RE2-R	50.1	2.85	3.33
	RE3-R	22.3	2.04	2.72
Group 3	A4-Open-U	19.8	0.32	0.46
	A4-Open-R	33.5	2.50	2.50
	RE4-Open-U	21.7 - 28.2	0.46	0.46
	RE4-Open-R	37.4 – 44.4	2.50	2.50

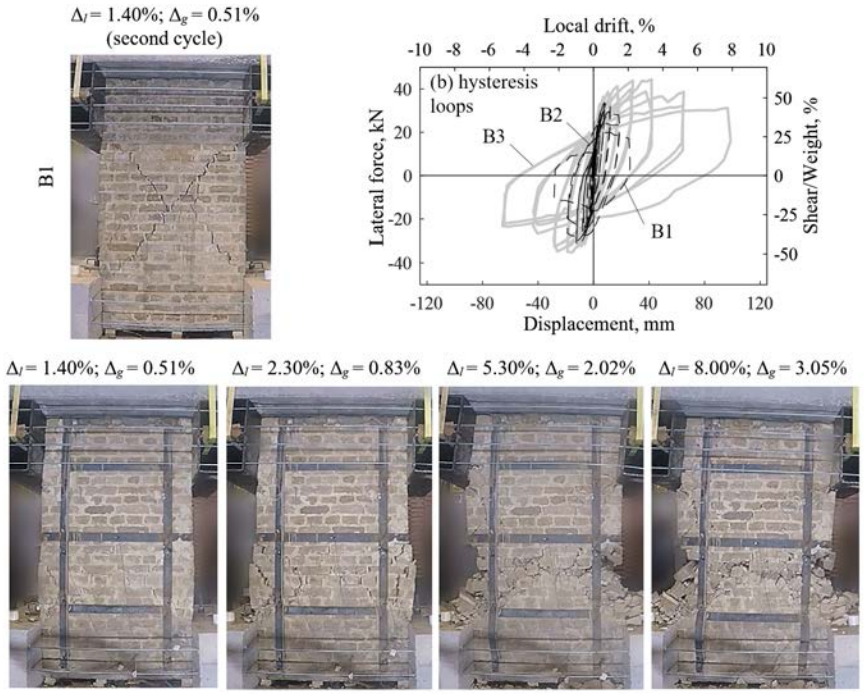

Fig. 3 – Representative results for Group 1 specimens.

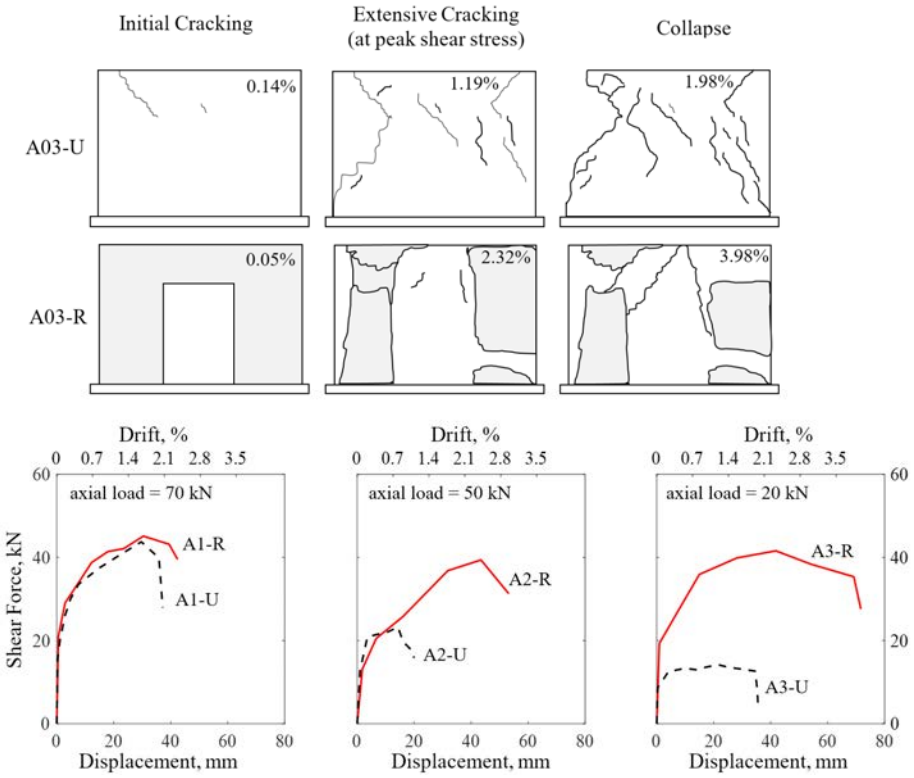

Fig. 4 – Representative results for adobe specimens in Group 2.

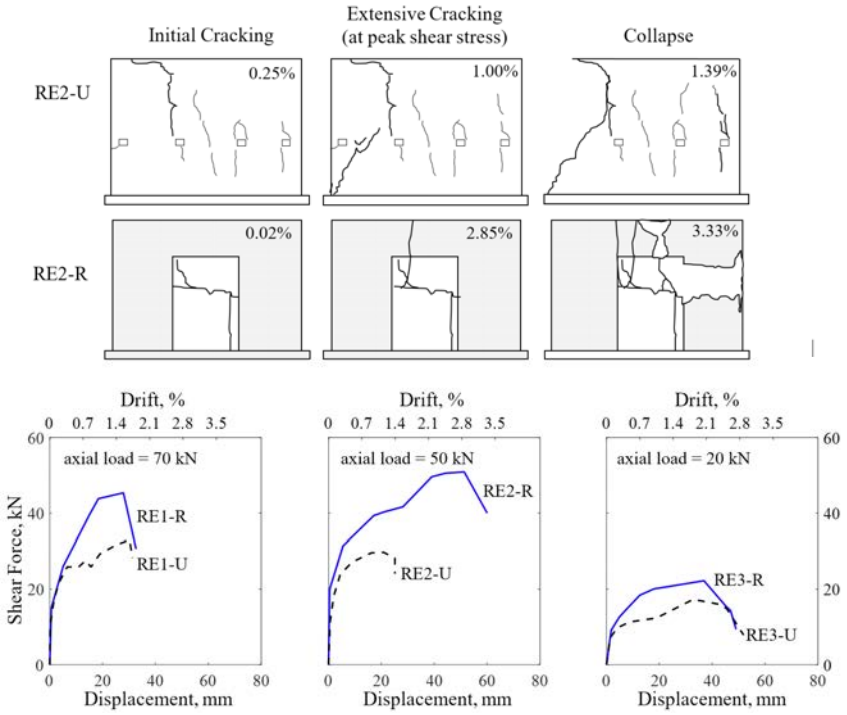

Fig. 5 – Representative results for RE specimens in Group 2.

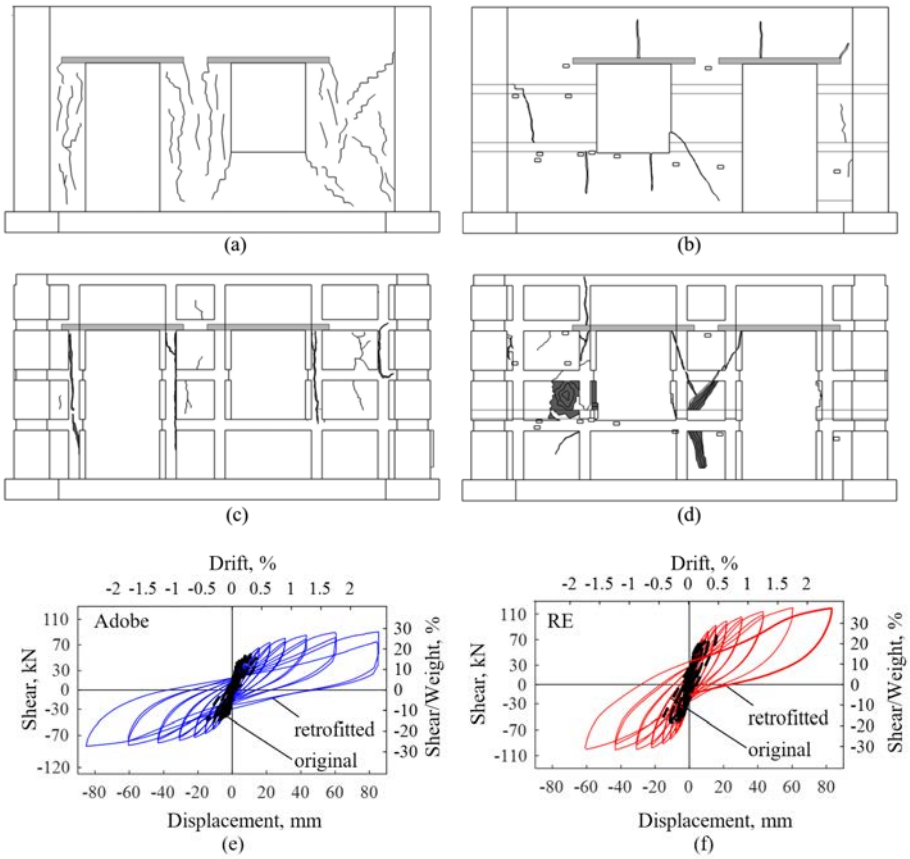

Fig. 6 – Representative results for Group 3 specimens. Cracking patterns of walls with openings: a) adobe wall bare 0.46% drift, b) RE wall bare 0.46% drift, c) adobe wall retrofitted 2.5% drift, d) RE wall retrofitted 2.5% drift. Cyclic response of: e) adobe specimens and f) RE specimens.

4.1 Damage Pattern

Fig. 3 depicts the failure modes of selected test specimens. In the unretrofitted Group 1 specimens (B1 and B2), observable shear cracks appeared at 0.90% drift; propagating from the bottom to the top corners mainly through the mud mortar joints, reaching crack widths of 20 mm at 1.4% local drift, in contrast to slight damage at the same drift level observed in the retrofitted specimen B3. Specimens B1 and B2 lost stability at 1.4% drift ratio while the B3 survived 2.3% before the onset of strength degradation and 5.3% drift ratio before severe damage and instability when the material located in the lower mid-height of the specimen suffered spalling at the edges, central diagonal cracks and buckling of vertical steel plates.

The Group 2 unretrofitted walls damage pattern observed in adobe and RE walls at the onset of initial cracking, extensive cracking, and near collapse limit states (as shown in Figs. 4-5) reveals some interesting behavior. The damage pattern of the adobe walls was highly distinct from that of RE walls. Diagonal dispersed cracks are observed in the adobe specimens; usually starting at the the top corners and propagate diagonally to the center of the specimen. The walls are gradually divided in three or four large blocks that eventually fall off as a collapse mechanism. For the RE walls, the cracking pattern is characterized by vertical cracks that propagates diagonally to the bottom corners of the walls. The collapse mechanism of the RE wall is reached by out-of-plane instability of a large wall segment between cracks. For both sets of tests, the higher vertical load tends to increase the number of cracks. Higher axial loads delayed the first crack initiation to higher drift levels of both the unretrofitted and the retrofitted adobe walls. However, higher axial loads did not have a significant effect on the drift demands corresponding to moderate and extensive damage. The Group 2 FSWM retrofitted adobe specimens' damage pattern at the peak strength was characterized by debonding of the stucco, exposure of the flexible wire mesh, and crack propagation. Very wide cracks were

observed in the unreinforced portions of the walls, highlighting a serious limitation of the partial retrofitting technique. Using FSWM retrofit did not prevent the onset of first cracking for thick adobe walls; on the contrary, it seems to accelerate it. The FSWM retrofit, however, is efficient delaying the occurrence of extensive damage, especially for low and moderate axial loads. Similar to adobe walls, the FSWM retrofit did not inhibit damage to the RE walls in Group 2, but only prevented local failures. No clear relation among drift capacity and axial load was observed for the retrofitted walls. During the tests, it was observed that the main function of the flexible steel welded wire mesh was to prevent wall segments from collapsing. Once first cracking occurs, the lateral stiffness of earthen wall decreases significantly, and the flexible mesh is unable to compensate for that loss. Meshes, however, are efficient to enhance the overall drift and energy dissipation capacity of thick earthen walls.

For Group 3 specimens, initial cracking occurred at 0.06% and 0.08% global drift values for the adobe and RE unretrofitted walls, respectively. The loading continued for the unretrofitted specimens until a global drift value of 0.46%, slightly beyond the onset of strength loss. The damage of the adobe wall was manifested of distributed vertical cracks in the wall piers, especially in those with low aspect ratio. The RE wall cracking is distinctly different from adobe wall as it was exhibited as significant deep concentrated cracks rather than distributed ones, dividing the wall into distinct wall segments. New cracks in the retrofitted specimens were first observed at drift levels of 0.45% for the adobe wall and 0.32% for the RE wall. For such low level of drift demand, the secant stiffness has decreased by as much as 90%. Fig. 6 shows the crack patterns for the retrofitted adobe wall and the retrofitted RE wall respectively at a drift level of 2.5%. These crack patterns were markedly different between the two specimens, with the adobe wall exhibiting mostly vertical cracks concentrated on the piers between openings, falling of loose material near the base, while the RE wall had longitudinal and diagonal cracks.

4.2 Strength and Deformation

The top-right sub-plot of Fig. 3 depicts lateral force-drift hysteresis response for Group 1 walls. It is evident that the steel strap retrofit scheme was superior in enhancing both the strength and the drift capacity of the retrofitted wall B3. Nearly 33% shear strength enhancement and 400% drift enhancement was achieved before reaching the severe damage state and significant strength loss of wall B3 at 5.3% drift. Superior energy dissipation capacity of wall B3 attests to the effectiveness of the SS retrofit scheme.

The lower parts of Figs. 4 and 5 show the cyclic backbone curves of Group 2 walls. It is clear that axial load increases the lateral load capacity of the unretrofitted earthen walls, likely due to reduced principal tension stresses. However, the shear capacity of the retrofitted adobe wall did not increase with the axial load. The retrofitted adobe walls' shear capacity was 30-50% higher than the diagonal tension capacity of the adobe prisms, while only one of the bare walls exceeded the adobe prism strength. It is evident from Fig. 4 that FSWM retrofit enhances the overall lateral response of the adobe walls only for low levels of axial load. The shear strength of the walls under low axial load increased by almost threefold while the drift at the maximum strength increased from 1.2% to 2.3%. For the moderate axial load, the shear strength increased from 23 to 39 kN/m^2, while the drift capacity at peak stress increased from 0.8% to 2.4%. However, for the high of axial load, neither the strength nor the drift capacity were positively impacted by using the FSWM. Combining this with damage pattern observations presented earlier, it seems there is a limitation of this retrofit method to be restricted to one story buildings with low to moderate seismicity. The lateral capacity of the RE walls was minimally enhanced with the FSWM retrofit, not as much as in the adobe walls. For the low axial load, the shear strength increased from 17 to 22 kN/m^2, but the drift capacity only increased from 1.8 to 2.0%. For an axial load of 50 kN, the lateral capacity increased by nearly 70%, while the drift capacity increased by nearly three-fold with the FSWM retrofit. The effect of the axial load to increase the shear capacity of the walls was less significantly in RE retrofitted walls.

The lower part of Fig. 6 shows the cyclic displacement versus lateral loads of Group 3 walls. In both unretrofitted walls, the strength started to degrade at 0.46% drift, but with no failure and only repairable damage. The adobe wall exhibited an approximately equal shear strength of 19.8 kN/m^2 in both directions, while the RE wall had shear strength of 28.2 kN/m^2 in the push and -21.7 kN/m^2 in pull directions. The

higher lateral load and diagonal tension capacity of the RE can be attributed to its higher compaction. Furthermore, the RE wall is made of large blocks and thus has much fewer failure planes than the adobe wall. In addition, the mortar used to attach the adobe was weak (made of water and earth only). These strengths were consistently smaller than the diagonal tension strength of the material characterization assemblies which had median values of 27 kN/m^2 for adobe and 31 kN/m^2 for RE (Section 2). The different aspect ratio of piers in the wall specimens can lead to additional modes of failure and crack patterns that cannot be captured with diagonal tension tests. The RE wall also had wider hysteretic loops as compared to the adobe wall, thus, indicating superior energy dissipation capacity.

Fig. 6 also shows the hysteretic response of the Group 3 retrofitted walls. Clearly, TSPR retrofit scheme significantly improved the strength and deformation capacity of the earthen walls. In both cases, the retrofitted specimens achieved a drift of nearly 2.5% prior to decay in the lateral load, resulting in an increase of over fivefold in the displacement capacity. The retrofitted adobe wall had the lateral strength of capacity of 33.5 kN/m^2 in both the push and pull directions, an increase of about 70% in compared to the original wall. The RE wall lateral strength was 44.4 kN/m^2 and 37.7 kN/m^2 in the push and pull directions, respectively. Thus, TSPR retrofit scheme enhanced the lateral load capacity of the RE wall by 57% to 72%. Thus, the TSPR scheme seems a more effective alternative compared to the FSWM scheme, but less superior than the SS scheme.

5. Conclusions

Earthen wall buildings constitute the largest majority of housing units worldwide, housing about one-third of world's population, many in regions of moderate and high seismicity. Besides, considerable percentage of world's heritage construction is made of earthen walls. Yet, research studies characterizing the seismic behavior of thick earthen walls are scare. This study presented the in-plane cyclic test results of a comprehensive test program featuring 19-full scale solid adobe and rammed earth walls tested under the effect of various influential parameters such as wall aspect ratio, axial load level, and window and door opening presence and three proposed retrofitting schemes. The retrofitting schemes featured steel straps, flexible steel welded wire meshes and timber straps combined with vertical post-tensioning rods. Test results of the unretrofitted walls show that the failure mechanisms are dominated by diagonal cracks dividing the walls into large segments that eventually spalled reducing shear capacity. It was found that the lateral capacity is controlled by the wall axial load and aspect ratio. Higher axial loads increased shear strength of the unretrofitted walls, but did not have a considerable effect on the strength of the retrofitted walls. The unretrofitted walls had limited drift capacity at peak strength with a lower bound of 0.8% while the retrofitted walls could reach a peak strength drift ratio exceeding 2%. Steel straps retrofit scheme increased adobe wall lateral strength and deformation capacity by 30% and 380%, respectively, allowing drift capacity at severe damage to reach 5.3%. Flexible steel wire mesh marginally increased shear strength of adobe walls under high axial load, while it was efficient enhancing lateral strength under low axial load by about 3 times, in contrast to an average strength enhancement of 42% in RE walls. However, the flexible steel wire mesh was ineffective in enhancing drift capacity of both adobe and RE walls under high axial loads, while it improved the adobe wall drift capacity by 2-3 times. Thus, the authors recommend limiting the use of steel wire mesh retrofit to one-story buildings in regions of low seismicity. The third retrofit solution (vertical and horizontal timber straps along with post-tensioned rods) provided superior performance to the retrofitted adobe and RE walls with openings, enhancing the lateral strength of the walls by 70%. Moreover, it increased the drift capacity of both adobe and RE walls with openings by more than 5 times, reaching 2.5% drift ratio without considerable damage. The steel straps retrofit scheme seems to be the most effective retrofit alternative followed by the timber straps with post-tensioning rods in seismic retrofitting of earthen walls in moderate to high seismicity.

6. Acknowledgements

The authors are thankful to members of the AIS-600 committee, especially to Santiago Rivero, Oscar R. Becerra, and Ismael Santana, for serving as technical advisors and reviewers of this research. Financial support was provided by AIS and Dirección de Patrimonio del Ministerio de Cultura and Instituto Distrital de Patrimonio Culturalof the Republic of Colombia. Gratitude is also due to the staff of the Material and Civil Works Research Center and the Civil Engineering Laboratory at Universidad de los Andes in Bogotá. The authors appreciate the contributions of Jose G. Martinez to the steel plates retrofitting alternative.

7. References

[1] Houben H, Guillard H (2008): Earth construction: a comprehensive guide. London, England; ISBN-13: 978-1853391934.

[2] Avrami E, Guillaud H, Hardy M (2008): Terra literature review an overview of research in earthen architecture conservation. The Getty Conservation Institute, Los Angeles, CA

[3] UNESCO World Heritage Centre AU (2012): World Heritage Earthen Architecture Programme Progress Report of Activities, 2007- 2012.

[4] Blondet M, Villa Garcia G, Brzev S, Rubiños Á (2011): Earthquake-Resistant Construction of Adobe Buildings: A Tutorial. *EERI/IAEE World Hous Encycl*, **56**:13–21. doi:10.1227/01.NEU.0000255422.86054.51.

[5] Liu K, Wang M, Wang Y (2015): Seismic retrofitting of rural rammed earth buildings using externally bonded fibers. *Constr Build Mater*, **100**:91–101. doi: 10.1016/j.conbuildmat.2015.09.048

[6] Bakhshi A, Ghannad MA, Yekrangnia M, Masaeli H (2017): Shaking table tests on dome-roof adobe houses. *Earthquake Eng Struct Dyn*, **46**:467–490. doi: 10.1002/eqe.2800

[7] Charleson A, Blondet M (2012): Seismic reinforcement for adobe houses with straps from used car tires. *Earthquake Spectra,* **28**:511–530. doi: 10.1193/1.4000014

[8] Sathiparan N, Mayorca P, Meguro K (2012): Shake table tests on one-quarter scale models of masonry houses retrofitted with PP-band mesh. *Earthquake Spectra*, **28**:277–299. doi: 10.1193/1.3675357

[9] Miccoli L, Müller U, Pospíšil S (2017): Rammed earth walls strengthened with polyester fabric strips: Experimental analysis under in-plane cyclic loading. *Constr Build Mater*, **149**:29–36. doi: 10.1016/j.conbuildmat.2017.05.115.

[10] Reyes JC, Yamin LE, Hassan WM, Sandoval JD, Gonzalez CD, Galvis FA (2018): Shear behavior of adobe and rammed earth walls of heritage structures. *Engineering Structures*, **174**: 526-537.

[11] Reyes JC, Rincon R, Yamin LE, Correal JF, Martinez JG, Sandoval JD, Gonzalez CD, Ange CC (2020): Seismic retrofit of existing earthen structures using steel plates, **230**:117039.

[12] Reyes JC, Smith-Pardo JP, Yamin LE, Galvis FA, Angel CC, Sandoval JD, Gonzalez CD (2019): Seismic experimental assessment of steel and synthetic meshes for retrofitting heritage earthen structures. *Engineering Structures*, **198**:109477.

[13] Reyes JC, Smith-Pardo JP, Yamin LE, Galvis FA, Sandoval JD, Gonzalez CD, Correal JF (2019): In-plane seismic behavior of full-scale earthen walls with openings retrofitted with timber elements and vertical tensors. *Bulletin of Earthquake Engineering*, **17**(7): 4193-4215.

[14] FEMA 461 (2007): Interim Testing protocols for determining the seismic performance characteristics of structural and nonstructural components. FEMA, Washington DC, USA.

